

Simultaneous Generation of UV at 411 nm and Red at 671 nm in a Dual-Structure Periodically Poled LiTaO₃ Crystal

X.-W. Fan^a, J.-L. He^{a, b, *}, H.-T. Huang^a, J.-L. Xu^b, X.-P. Hu^c, and S.-N. Zhu^c

^a College of Physics and Electronics, Shandong Normal University, Ji'nan, 250014 China

^b Key Laboratory of Crystal Materials, Shandong University, Ji'nan, 250100 China

^c National Laboratory of Solid-State Microstructures, Nanjing University, Nanjing, 210093 China

*e-mail: jlhe@sdu.edu.cn

Received May 28, 2008; in final form, June 6, 2008

Abstract—A dual-color laser of red at 671 nm and ultraviolet (UV) at 411 nm was generated from dual-wavelength fundamental waves at 1342 and 1064 nm with a single periodically poled LiTaO₃ (PPLT) optical superlattice. The PPLT sample used consists of two segments in a series: the first segment has a period of 14.55 μm for the second-harmonic generation (SHG) of 1342 nm and the second segment has periods of around 10.3 μm for the generation of UV light by sum-frequency mixing (SFG) of 1064 and 671 nm. An average output power of 3 and 79 mW for UV and red, respectively, has been obtained.

PACS numbers: 42.65.Ky, 42.55.Xi, 42.60.Gd

DOI: 10.1134/S1054660X08110200

1. INTRODUCTION

Photodynamic therapy (PDT) increasingly used in the modern tumor medical field is one of the new comparatively more selective and nontoxic methods of treating patients with malignant tumors of different cellular types [1–7]. PDT is most commonly performed by intravenous administration of photosensitizers, such as hematoporphyrin derivative (HPD) or porphyrin derivatives, selectively retained by malignant tumors. Subsequent photoexcitation with UV-blue (405–488 nm) light causes fluorescence, which is useful for diagnosis, and, then, excitation by red light destroys the cancer tissue. Because the longer energy wavelengths exhibit a deeper penetration into biological tissues and a more effective treated tumor volume [8, 9], the 600–800-nm spectral band was usually used as therapeutic light in PDT. The new photosensitizers, such as ZnPcS₂P₂ [10] and BPD-MA [11], absorb wavelengths at around 670 and 690 nm [12].

At present, the available coherent sources used in PDT were a 406.7–422.6-nm krypton ion laser, a 457.9–514.5-nm argon ion laser, a gold vapor laser, a copper vapor laser, a 630-nm dye laser pumped by an argon ion laser, and a 630-nm laser diode. But, gas lasers have many disadvantages including a short lifetime, a low reliability, a large size, a high energy consumption, and high expenses for maintenance, while the laser diode has a poor beam quality. Furthermore, there are very few laser options at present for supplying excitation and a therapeutic light source simultaneously. The nonlinear optical frequency conversion of solid-state lasers operating in the near-infrared range is a very effective method for UV- and red-light generation. But, there was difficulty in obtaining the UV light

around 410 nm by the simply frequency conversion besides the optical parametric oscillator method.

In this paper, we report on the design and simultaneous generation of red- and UV-light at 671 and 411 nm, respectively, based on single-pass quasi-phase-matched (QPM) SHG and SFG processes in a single PPLT from Q-switched, diode-end-pumped Nd:YVO₄ lasers operating at the 1342 and 1064 nm fundamental waves, respectively. The UV output power of 3 mW and the red output power of 79 mW were obtained. The UV light which coincides with the optimal excitation wavelength can be used for tissue diagnosis and the red light which coincides with the optimal absorption wavelength can be used for therapeutic light. Furthermore, the efficiency of the PDT with a Q-switched laser is better than with the continuous-wave laser [13] and one machine satisfies the needs of diagnosis and therapy of malignant tumors simultaneously.

2. DESIGN AND FABRICATION OF THE QPM CRYSTAL

QPM always permits noncritical phase matching and the use of the large diagonal nonlinear coefficients, which are inaccessible with birefringent phase matching, and optical superlattices, such as periodically poled LiNbO₃ (PPLN) and PPLT [14], have been becoming attractive materials for nonlinear optical frequency conversion by QPM. To obtain an efficient output of 671 and 411 nm, respectively, a key problem is to design and fabricate a QPM crystal, by which two reciprocals should be provided to phase match the two nonlinear processes described here. The first one is the SHG of 1342 nm to generate red light at 671 nm, the

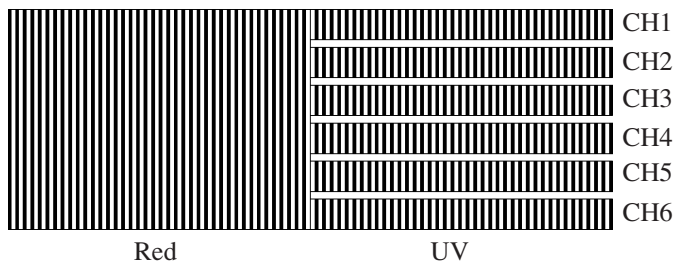


Fig. 1. Sketch of the QPM structure of the PPLT sample.

second is the SFG of 1064 and 671 nm to generate UV light at 411 nm. For this purpose, a PPLT device consisting of two segments in a series forming a cascaded structure was used in our experiment. The first-order reciprocal was used in the SHG process for the most efficient nonlinear conversion. Because the QPM conditions of the SHG and third-harmonic generation with a first-order reciprocal of a PPLT at a temperature of 74.1°C can be simultaneously satisfied at the fundamental wavelength of 1342 nm [15] and the photorefractive effects on the frequency conversion process was serious at lower temperatures, we preset the operating temperature at 150°C. As a result, the nominal period of the first segment was 14.55 μm calculated using the temperature-dependent Sellmeier equation from [16]. If a first-order QPM was also used in the SFG process, the grating period was too small to fabricate a bulk sample with a thickness of 0.5 mm by poling. Furthermore, the duty cycle of 0.5 forbids the choice of a second-order reciprocal, we choose the third-order reciprocal for the SFG process. There are some uncertainties in the coefficients of the Sellmeier equation and fabrication errors of the domain pattern may arise, whereby the second segment was designed in six parallel channels. The structure of the PPLT sample was shown schematically in Fig. 1. The channels were 1 mm wide with different periods ranging from 10.301 to 10.332 μm with a step of 0.0063 μm , which correspond to temperature from 138 to 148°C and a step of 2°C. These channels ensure that the phase matching of the SFG process could be accomplished by selecting a suitable channel for the laser beam. The two segments were arranged in a series and fabricated in the same LiTaO₃ (LT) wafer by using the conventional electrical poling technique at room temperature. The wafer was 0.5 mm in thickness, and the lengths of the two segments were 20 and 15 mm, respectively. The two end faces of the sample were optically polished, but not coated.

3. FUNDAMENTAL LIGHT SOURCE

The Nd:YVO₄ crystal has been identified as one of the promising materials for a diode-pumped solid-state laser because of its high absorption over a wide pumping wavelength bandwidth, large stimulated-emission

cross sections at both 1342 and 1064 nm, and its polarized output [17]. Its emission cross section at 1342 nm was roughly equal to that of the 1064-nm transition in Nd:YAG [18], which were beneficial for the efficient generation of a 1342-nm emission and its frequency-doubling red light at 671 nm. The thermal effect in the laser crystal has a serious effect on the resonator stability, the optimum resonator mode size, and the frequency conversion efficiency. For low doping, the reduced absorption coefficient at the pump wavelength permits the deposited heat to be spread along the axis of the laser crystal, which results in a reduction in the heat load, and a consequent thermal effect [19, 20]. Thus, a Nd:YVO₄ crystal with a 0.3 at % Nd³⁺ concentration as the active medium was chosen to generate a 1342-nm fundamental wave.

Another key problem is achieving the Q-switched simultaneous dual-wavelength operation at 1064 and 1342 nm with an optimal spatial overlap. Dual-wavelength outputs with a good temporal and spatial overlap can be obtained by adjusting the open time offset of the two Q switches, the ratio of the cavity lengths according to their emission cross sections or by using the characteristic polarization-dependent emission cross section of the active medium [21–23]. But, the conditions were obtained by assuming that the cavity losses were constant. In fact, the diffraction losses arising from thermally induced spherical aberration were a function of the pump power [24]. Even then, there was difficulty in obtaining the dual-wavelength lasing with a good laser performance and stabilization due to the technical problem in the coating process.

A composite resonator was used and the experimental setup is presented schematically in Fig. 2. The pump sources were fiber-coupled laser diodes with a core diameter of 1.15 and 400 μm , the pump radii in the crystals were around 350 and 200 μm , respectively. The two Nd:YVO₄ crystals, with the dimensions 4 × 4 × 8 mm, were mounted in copper blocks cooled by the water at a temperature of 18°C. In order to reduce the cavity loss, both sides of gain crystal 1 were coated for antireflection (AR) at 1064 nm ($R < 0.2\%$) and a high transmission (HT) at the pump light 808 nm ($R > 0.5\%$), and both sides of gain crystal 2 were coated for AR at 1342 nm ($R < 0.2\%$), AR at 1064 nm ($R < 0.2\%$), and HT at 808 nm ($R < 0.5\%$). Input mirror M_1 was a flat mirror with AR at the pump wavelength on the entrance face and with a high-reflection coating (HR) at 1064 nm ($R > 99.8\%$) and HT at the pump light ($T > 95\%$) on the second surface. Input mirror M_2 has a 1000-mm radius of a curvature concave mirror with AR at the pump wavelength on the entrance face and with a high-reflection coating (HR) at 1342 nm ($R > 99.8\%$), HT at the pump light ($T > 95\%$), and HT ($T > 80\%$) at 1064 nm on the second surface in order to suppress lasing at the 1064-nm transition. Dichroic mirror M_3 , which was a plane mirror, permits separate 1342- and 1064-nm cavity arms. The output coupler (OC) was a

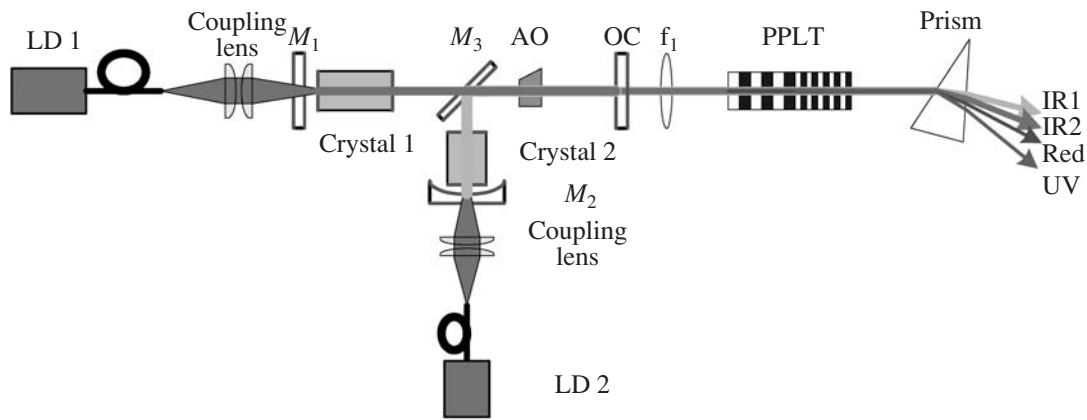


Fig. 2. Sketch of the experimental setup for the generation of UV and red light.

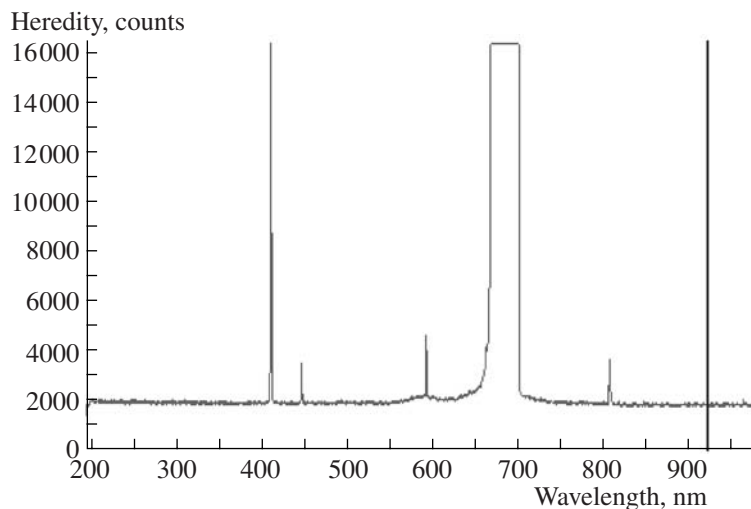


Fig. 3. Spectrum of the lasing lines of the UV and red dual-color laser.

plane mirror with a transmission of 3% for 1342 nm and 40% for 1064 nm, respectively. An acousto-optical (AO) Q-switch (NEOS) AR-coated $1.3 \mu\text{m}$ was inserted into the common cavity, the r.f. drive power was 50 W, and the repetition rate was variable from 1 to 50 kHz. The temporal and spatial overlap of the two outputs can be adjusted by controlling the pumping-power level and the position of pump source 1, so that the effect resulting from the accuracy of the coating of the output mirror can be reduced. In order to enhance the harmonic conversion efficiency, the fundamental waves were focused onto the PPLT sample by a lens with a focal length of 50 mm. The sample was heated in an oven for the phase-matching temperature with an accuracy of 0.1°C . The laser beams were separated at the output end with a prism and they were detected with a laser power meter (model FieldMax II, Coherent), respectively.

4. RESULTS AND DISCUSSION

When the incident pump power of LD 1 was 3.03 W, the incident pump power of LD 2 was 9.37 W and the

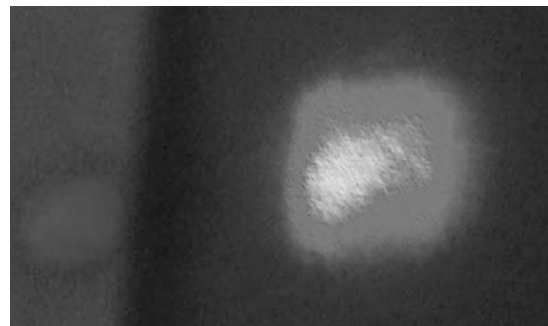


Fig. 4. The far-field shapes of the beam spot of the UV and red laser.

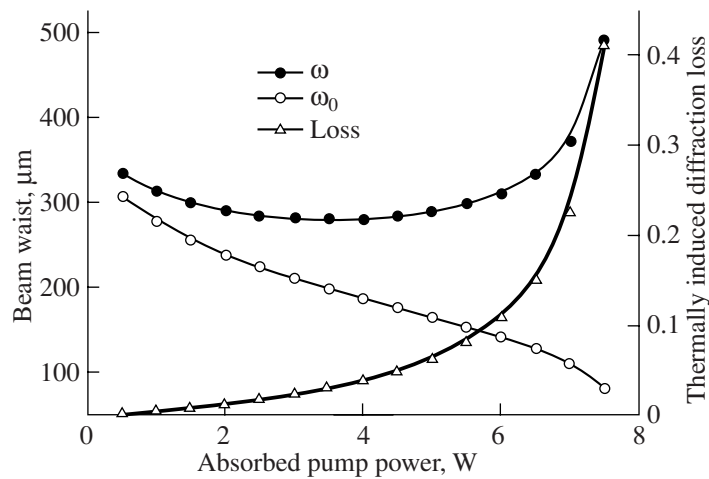


Fig. 5. Dependences of the relative thermally induced diffraction losses and the beam waist of the laser cavity mode at 1342 nm on the absorbed pump power.

repetition rate was 10 kHz. The optimum temporal overlap between the two wavelengths was obtained, the average output power was 210 mW for 1064 nm and 1.312 W for 1342 nm and the pulse widths were 23 and 29 ns, respectively. The average output power of 3 mW for UV light and 79 mW for red light have been obtained at the PPLT operating temperature of 144.7°C. The radiation spectrum of the UV and red dual-color laser has been recorded by spectrometers (model HR4000) and the result is shown in Fig. 3. The far-field shapes of the dual-color beam spot separated by a dispersive prism at the range of 100 cm behind the OC are shown in Fig. 4.

The output power of the UV and red light was below our expectations, even taking into account the Fresnel reflection on the front rear side of the PPLT and the diffraction loss of the prism. This may be caused for the following reasons. The first was related to the performance of the fundamental sources. In our experiment, the resonator lengths were about 113 mm for 1342 nm and about 103 mm for 1064 nm. Based on these experimental parameters and considering the thermal lens effect, the theoretical dependences of the relative thermally induced diffraction loss arising from the thermal effect of the laser crystal and the beam waist of the laser cavity mode at 1342 nm on the absorbed pump power have been calculated and the results were shown in Fig. 5. Obviously, the mode-to-pump ratio was larger than unity in the case of a slightly high pump power, while the optimum mode-to-pump ratio was about 0.8–1.0 [24]. Thus, the thermally induced diffraction loss was large and had a bad influence on the performance of the diode-end-pumped Nd:YVO₄ 1342-nm laser. Furthermore, a limit to our experimental condition is that the laser crystals and the pump sources used in our experiment were different, and the average output power for the two fundamental waves were low when

the optimum temporal overlap between the two wavelengths was obtained. The cavities and the pump sources should be optimized. The second reason lies in the fabrication process of the PPLT. The limited photolithographic precision leads to discrepancies in the light phase-matching temperatures. Missing domains can lead to a reduction in the effective nonlinear coefficient. All of these will reduce the output power and should be improved in further work.

5. CONCLUSIONS

In summary, all solid-state red light at 671 nm and UV light at 411-nm dual-color laser sources have been realized in a single dual-structure PPLT with multiple channels based on a single-pass QPM SHG of 1342 nm and SFG of 1064 and 671 nm from dual-wavelength fundamental waves at 1342 and 1064 nm, respectively. The average output power was about 3 mW for UV light and 79 mW for red light. This scheme can be an attractive way to obtain the efficient and compact UV and red coherent source. Further work to obtain a higher power and efficiency of UV and red lasers is under way. We believe that the UV–red dual-color laser can be used in PDT.

ACKNOWLEDGMENTS

This work was supported by the Grander Independent Innovation Project of Shandong Province (grant no. 2006GG1103047), the National Natural Science Foundation of China (grant no. 60478009), and the Program for Taishan Scholars.

REFERENCES

1. P. F. C. Menezes, V. S. Bagnato, R. M. Johnke, et al., "Photodynamic Therapy for Photogem and Photofrin

- Using Different Light Wavelengths in 375 Human Melanoma Cells,” *Laser Phys. Lett.* **4**, 546–551 (2007).
2. J. Ferreira, L. T. Moriyama, C. Kurachi, et al., “Experimental Determination of Threshold Dose in Photodynamic Therapy in Normal Rat Liver,” *Laser Phys. Lett.* **4**, 469–475 (2007).
 3. J. Ferreira, C. Kurachi, L. T. Moriyama, et al., “Correlation between the Photostability and Photodynamic Efficacy for Different Photosensitizers,” *Laser Phys. Lett.* **3**, 91–95 (2006).
 4. P. F. C. Menezes, H. Imasato, J. Ferreira, et al., “Aggregation Susceptibility on Phototransformation of Hematoporphyrin Derivatives,” *Laser Phys. Lett.* **5**, 227–235 (2008).
 5. C. Lochmann, T. Haeupl, and J. Beuthan, “Luminescence Lifetime Determination for Oxygen Imaging in Human Tissue,” *Laser Phys. Lett.* **5**, 151–155 (2008).
 6. J. Ferreira, P. F. C. Menezes, C. Kurachi, et al., “Photostability of Different Chlorine, Photosensitizers,” *Laser Phys. Lett.* **5**, 156–161 (2008).
 7. J. Ferreira, P. F. C. Menezes, C. Kurachi, et al., “Comparative Study of Photodegradation of Three Hematoporphyrin Derivative: Photofrin, Photogem, and Photosan,” *Laser Phys. Lett.* **4**, 743–748 (2007).
 8. Wai-Fung Cheong, S. A. Prahl, and A. J. Welch, *IEEE J. Quantum Electron.* **26**, 2166 (1990).
 9. R. D. Barabash, J. S. McCaughan, Jr., A. S. Kolobanov, et al., *IEEE J. Quantum Electron.* **26**, 2226 (1990).
 10. Huang Jin-Ling, Chen Nai-Sheng, Huang Jian-Dong, et al., *Sci. China B* **44**, 113 (2001).
 11. Chen Jie-Bo, OU Min-Rui, Li Zong-Qin, and XU Xiao-Ping, *J. Strait Pharmaceutical* **15**, 8 (2003).
 12. Wang Yong, Li Zheng-Jia, Zhu Chang-Hong, and Chen Zhi-Chu, *J. Laser* **24**, 81 (2003).
 13. Li Xiao, Wu Yu-Fen, and Li Feng, *Chin. J. Cancer Prev. Treat.* **14**, 1117 (2007).
 14. Shi-Ning Zhu, Yong-Yuan Zhu, and Nai-Ben Ming, *Science* **278**, 843 (1997).
 15. G. Z. Luo, S. N. Zhu, J. L. He, et al., *Appl. Phys. Lett.* **78**, 3006 (2001).
 16. J. P. Meyn and M. M. Fejer, *Opt. Lett.* **22**, 1214 (1997).
 17. G. J. Kintz and T. Baer, *IEEE J. Quantum Electron.* **26**, 1457 (1990).
 18. A. W. Tucker, M. Birnbaum, C. L. Fincher, and J. W. Erler, *J. Appl. Phys.* **48**, 4907 (1977).
 19. A. Di Lieto, P. Minguzzi, A. Pirastu, et al., *Appl. Phys. B* **75**, 463 (2002).
 20. A. Di Lieto, P. Minguzzi, A. Pirastu, and V. Magni, *IEEE J. Quantum Electron.* **39**, 903 (2003).
 21. A. George and J. Henderson, *Appl. Phys.* **68**, 5451 (1990).
 22. W. X. Lin and H. Y. Shen, *J. Appl. Phys.* **86**, 2979 (1999).
 23. W. X. Lin, S. Q. Lin, and J. H. Huang, *J. Opt. Soc. Am. B* **20**, 479 (2003).
 24. Y. F. Chen, T. M. Huang, C. F. Kao, et al., *IEEE J. Quantum Electron.* **33**, 1424 (1997).